Development 128, 1731-1744 (2001)
Printed in Great Britain © The Company of Biologists Limited 2001
DEV2671

The dermomyotome dorsomedial lip drives growth and morphogenesis of both the primary myotome and dermomyotome epithelium

Charles P. Ordahl*, Eli Berdougo‡, Sara J. Venters and Wilfred F. Denetclaw, Jr§

Department of Anatomy and Cardiovascular Research Institute, University of California San Francisco, San Francisco, CA 94143, USA

‡Present address: Skirball Institute of Biomolecular Science, New York University School of Medicine, 540 First Avenue, New York, NY 10016, USA

§Present address: Department of Biology, San Francisco State University, San Francisco, CA 94132, USA

*Author for correspondence (e-mail: ordahl@itsa.ucsf.edu)

Accepted 5 March; published on WWW 19 April 2001

SUMMARY

The cellular and molecular mechanisms that govern early muscle patterning in vertebrate development are unknown. The earliest skeletal muscle to organize, the primary myotome of the epaxial domain, is a thin sheet of muscle tissue that expands in each somite segment in a lateral-to-medial direction in concert with the overlying dermomyotome epithelium. Several mutually contradictory models have been proposed to explain how myotome precursor cells, which are known to reside within the dermomyotome, translocate to the subjacent myotome layer to form this first segmented muscle tissue of the body. Using experimental embryology to discriminate among these models, we show here that ablation of the dorsomedial lip (DML) of the dermomyotome epithelium blocks further primary myotome growth while ablation of other dermomyotome regions does not. Myotome growth and morphogenesis can be restored in a DML-ablated somite of a host embryo by transplantation of a second DML from a donor embryo. Chick-quail marking experiments show that new myotome cells in such recombinant somites are derived from the donor DML and that cells from other regions of the somite are neither present nor required. In addition to the myotome, the transplanted DML also gives rise to the dermomyotome epithelium overlying the new myotome growth region and from which the mesenchymal dermatome will later emerge. These results demonstrate that the DML is a cellular growth engine that is both necessary and sufficient to drive the growth and morphogenesis of the primary myotome and simultaneously drive that of the dermomyotome, an epithelium containing muscle, dermis and possibly other potentialities.

Key words: Muscle patterning, Chick/quail chimera, Somite, Dermatome, Confocal microscopy, Fate mapping

INTRODUCTION

The first differentiated skeletal muscle cells to appear during early vertebrate development are those of the epaxial myotome, the segmented embryonic primordia of the skeletal muscles of the body axis (Brand-Saberi and Christ, 2000). At least three phases of epaxial myotome development can be distinguished although there may be more. During the first phase, which we denote as 'primary' myotome development, a thin sheet of muscle is formed immediately beneath the epithelial dermomyotome in each somite segment (Fig. 1). Differentiated myocytes in the primary myotome are post-mitotic, highly differentiated, mononucleate myofibers that are arrayed in side-by-side fashion (Holtzer et al., 1957) spanning the craniocaudal width of every somite segment (100-200 μm; see Fig. 1A). The primary myotome rapidly expands along the mediolateral axis of the somite (Fig. 1B), in concert with the expansion of the dermomyotome epithelium (Denetclaw et al., 1997; Denetclaw and Ordahl, 2000). Once primary myotome expansion is underway, a second phase of development ensues which involves appositional growth of each myotome segment through addition of new fibers in a superficial-to-deep direction (Fig. 1C; Kahane et al., 1998a; Denetclaw and Ordahl, 2000). Throughout its primary and secondary phases, the fibers of the epaxial myotomes span only a single somite segment. Formation of multi-segmental back muscles constitutes a third phase, or more properly, onset of the first of many later stages of epaxial muscle development that involve much later, and possibly more complex tissue interactions. Moreover, the extent to which primary and secondary myotome fibers become incorporated into multinucleate myotubes, which begin to appear in the epaxial domain at embryonic day of gestation (ED) 3 in chick embryos and at ED11.5 in mouse embryos (Venters et al., 1999), remains unclear. A coherent model that accounts for the formation of epaxial muscle during all of these phases is not available but primary myotome formation has been a focus of recent investigation employing cellular, molecular and experimental embryological strategies.

The precursors that give rise to all skeletal muscle in the body are known to reside in the somites (Christ et al., 1974;

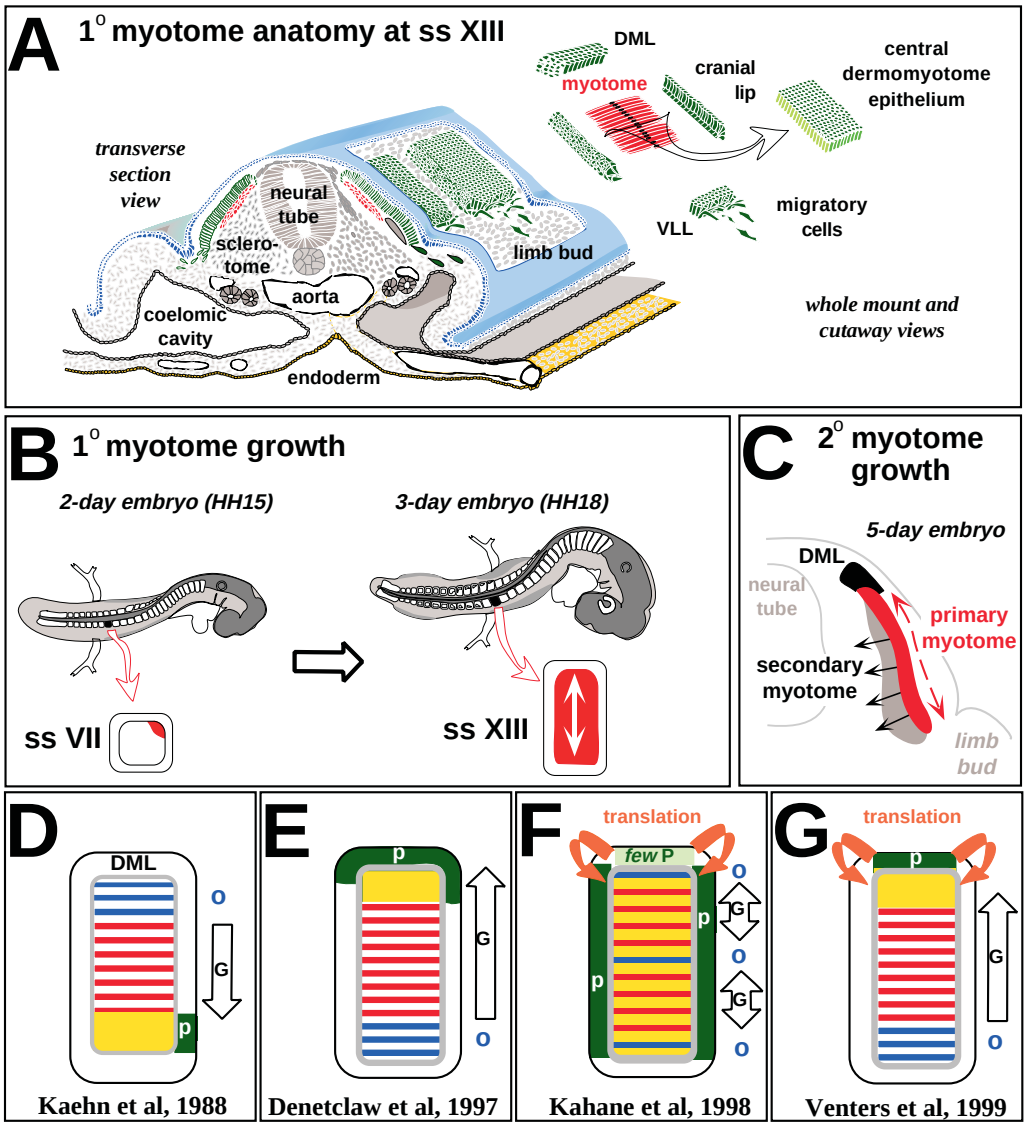

Fig. 1. Models of primary myotome formation in amniote embryos. (A) Cross section and perspective illustration of ss XIII wing level somites showing the thin primary myotome (red) immediately subjacent to the dermomytome (green), The position of the DML is indicated as are the migratory cells that form limb muscle. (B) Somitogenesis and primary myotome growth. The development of the primary myotome in one somite segment at the wing level is illustrated from its beginning in a 2-day embryo to an intermediate stage of development in a 3-day embryo. The first myotome cells (red) are detected in the craniomedial corner of a stage VII somite (ss VII) and by ss XIII, the myotome has grown to span most of the craniocaudal and mediolateral extent of the somite. (C) Position of the secondary myotome. As the primary myotome (red) expands mediolaterally, a secondary wave of myotome formation occurs immediately beneath it (grey). (D) Four recent models of myotome formation. In each the position of the oldest myotome fibers (blue, o), and ongoing myotome precursor cell activity (green, p) is indicated. The predicted growth direction for the myotome (G) is indicated by the white arrows labeled G. Blue lines indicate the oldest myotome fibers, while red lines indicate myotome fibers born later. In F, the light green area labeled 'few P' denotes a prediction of precursors within DML which make a minor contribution to myotome growth and morphogenesis. Orange arrows indicate translation of precursor cells within the dermomyotome epithelium prior to translocation to the myotome layer. Yellow indicates regions in the myotome layer where nascent (elongating) myotome cells are expected to be located. In this and all subsequent figures, the medial direction is towards the top of the figure and cranial is to the right. Other abbreviations: DML, dorsomedial lip; DM, dermomyotome; VLL, ventrolateral lip; HH, Hamburger Hamilton stage; ss, somite stage.

Chevallier et al., 1977; and reviewed by Brand-Saberi and Christ, 2000). Precursors of the epaxial myotome reside within the medial half of the dermomyotome epithelium (Ordahl and Le Douarin, 1992; Denetclaw et al., 1997; Williams and Ordahl, 1997) while limb muscle precursors lie within its lateral half (Williams and Ordahl, 1994; Williams and Ordahl, 2000). Limb muscle precursor cells migrate over long distances before differentiating in the limb bud (Christ et al., 1974; Chevallier et al., 1977). Nascent myotome cells, in contrast, differentiate in situ after undergoing 'myotomal translocation', a specialized form of morphogenetic cell movement in which cells from the dermomyotome epithelium are displaced into the subjacent myotome layer. Although myotomal translocation was hypothesized as early as the nineteenth century (Fischel, 1895; Williams, 1910), precise information regarding the nature of that translocation process has been lacking. In wing-level somites the first differentiated myotomal myocytes appear beneath the craniomedial corner of the dermomyotome (Kaehn et al., 1988) at approximately somite stage XII (ss XII) (Fig. 1B). Subsequent addition of new myotome cells is a key issue in understanding and discriminating amongst models for myotome growth and morphogenesis.

Based upon morphometric analysis of the earliest myotomal myocytes formed in individual somites, Christ and coworkers (Kaehn et al., 1988) proposed that the site of new myotome cell addition was asymmetric, chiefly along the cranial edge of the dermomyotome and in a progressive medial-to-lateral sequence (see Fig. 1D). That model for myotome formation yielded several predictions. First, that the oldest myotome fibers (blue and designated 'o') would be located in the extreme medial margin of the epaxial myotome. Second, that the precursors for new myotome fibers (green, 'p') would be

located at the extreme craniolateral margin of the myotome. Third, that the epaxial myotome growth direction (arrow G) would be in a medial-to-lateral direction. By contrast, precursor-product analysis of myotome formation through the use of fluorescent lineage-tracing dyes (Denetclaw et al., 1997) indicated that myotome growth occurs in the opposite direction (lateral-to-medial) as a consequence of asymmetric addition of new myotome cells along the dorsomedial lip (DML) of the dermomyotome (Fig. 1E). A third model, based on a combination of thymidine dating and dye injection (Kahane et al., 1998b), suggests that the first myotomal myocyte cells that appear in the somite craniomedial corner act as 'pioneer cells' that define the morphogenetic aspects of future myotome growth by providing a scaffold for the symmetrical intercalation of new myofibers at the cranial and caudal lips of the dermomyotome epithelium (Fig. 1F). In this model, these first-born myocytes elongate to span the somite width and are then displaced in a mediolateral direction through intercalation of new myocytes that arise from precursor cells that are arrayed symmetrically, along both the caudal and cranial lips of the dermomyotome. A fourth model (Fig. 1G; Venters et al., 1999) based upon morphometric and gene expression analysis of mouse myotome development (the previous three models are based on analysis of avian development) predicts the same direction of myotome growth as the Denetclaw et al. model except that precursor cells are proposed to first translate from the DML to either the cranial or caudal dermomyotome lips prior to translocating to the myotome layer. The model in F also proposed a minor contribution by such transitional movements from the DML.

Although the models outlined above postulate diverse locations for myotome precursor cells, the first-born myotomal myocytes and different direction of myotome growth, no direct experimental evidence fully reconciles their observational differences. While dye-lineage analysis (Denetclaw et al., 1997) showed that myotome precursor cells are abundant in the DML, a finding compatible with neither the Kaehn et al. model (Kaehn et al., 1988) nor the Kahane et al. model (Kahane et al., 1998b), dye-lineage analysis cannot account quantitatively for all of the myotome precursor cells and their myotomal progeny. Moreover, using embryo surgery to remove the DML, Kahane et al. concluded that the DML is dispensable for myotome growth and morphogenesis (Kahane et al., 1998). In order to discriminate among such observational differences, therefore, we have used a series of surgical experiments that combine experimental embryological approaches with dye-lineage analysis to analyze myotome formation. Site-specific ablation experiments were used to determine which portions of the dermomyotome epithelium are necessary for myotome growth and morphogenesis. Transplantation of quail dermomyotome donor fragments from active myotome generator regions into chick host embryos, and vice versa provided a means of determining which regions are sufficient to drive myotome growth and morphogenesis. The results demonstrate that cells contained within the somite DML are both necessary and sufficient for growth and morphogenesis of the primary myotome and that cells from other regions of the somite, including older regions of the myotome, are not required once DML activity is underway. Our results support the model for primary epaxial myotome formation of Denetclaw et al. (Denetclaw et al., 1997) and provide new information regarding the growth and patterning of the myotome and dermomyotome.

MATERIALS AND METHODS

Surgical ablations and transplantations

Chicken eggs (*Gallus domesticus*) and Japanese quail eggs (*Coturnix coturnix japonica*) were obtained from Petaluma Farms (Petaluma, CA) and from Strickland Quail Farms (Pooler, GA), respectively. After timed incubation at 39°C, embryo microsurgery and tissue transplantation experiments were performed as previously described (Williams and Ordahl, 1996; Ordahl and Christ, 1997; Williams and Ordahl, 2000) with the modifications noted below.

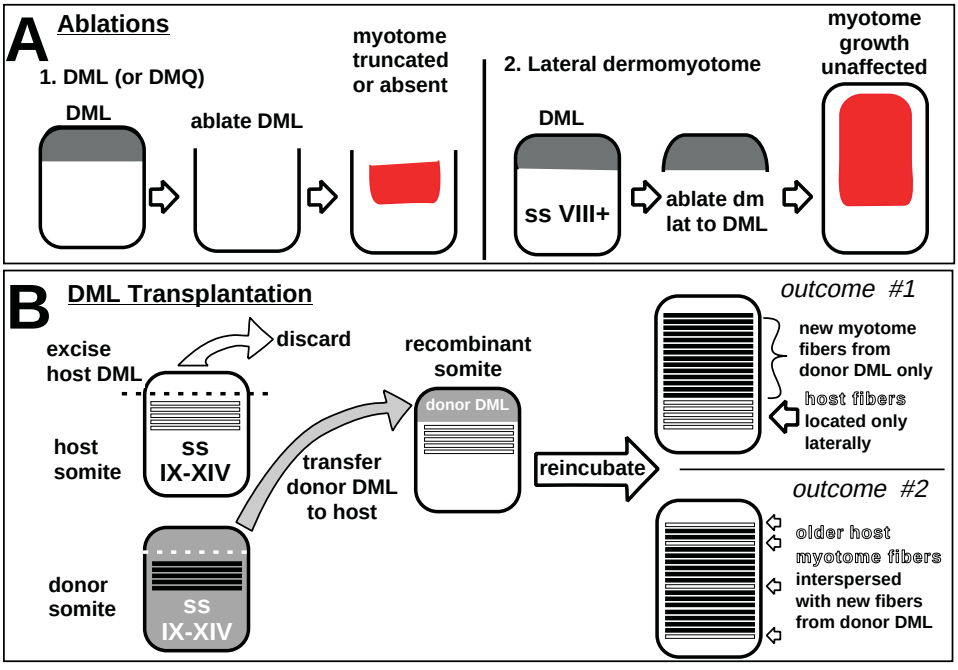

Fig. 2. Outline of experiments and outcomes. (A) 1. Ablation of the DMQ of somites <ss XI or the DML in somites >ss VIII results in cessation of further myotome growth as evidenced by medial truncation of the myotome. 2. Ablation of all the dermomyotome except for the DML results in normal myotome growth. (B) Transplantion of a donor DML to a host somite lacking a DML restores myotome growth. In hypothetical outcome #1, the new myotome generated by the DML is composed solely of donor cells. In hypothetical outcome #2, new myotome contains donor cells but also contains distributed host myotome fibers that are derived from older, lateral regions of the myotome.

For DML and dorsomedial quadrant (DMQ) ablations (illustrated in Fig. 2A), the dermomyotome epithelium was incised craniocaudally and slightly lateral to the DML. DML tissue fragments were then removed by mouth aspiration using a finely tapered glass micropipette (100 μl capacity) fashioned on a Flaming/Brown Micropipette Puller (P-87, Sutter Instrument Co). Lateral dermomyotome ablations were performed in similar fashion except that a second parallel cut was made lateral to the ventrolateral lip and medial to the Wolffian duct before freeing the lateral portion of the dermomyotome, which was subsequently removed by mouth aspiration. The surgical area was rinsed with Tyrode's solution, the egg sealed with Parafilm and incubated for 18-24 hours. In some cases fluorescent tracer dyes were injected to allow myotome fibers generated from the remaining somite fragments to be identified. Details of the ablation surgeries and their outcomes are shown in Table 1.

For DML transplantation (illustrated in Fig. 2B), donor (quail or chick) embryos were excised and pinned dorsal-side-up in black Sylgard-lined (Dow Corning) dissection dishes containing Tyrode's solution. To expose the DML, a cut was made through the ectoderm at the level of the wingbud or cervical somites (ss X-XX) and the dermomyotome layer was separated from the neural tube and underlying sclerotome by microscalpel teasing and brief pancreatin enzyme treatment. A craniocaudal incision made lateral to the DML region of the dermomyotome layer allowed the DML tissue fragment to be teased away from the embryo using microscalpels and then gently aspirated into a micropipette for transfer onto the blastoderm of a waiting host embryo (quail or chick) from which the DML of an equivalent stage somite had been previously removed. The donor DML was manoeuvred into position in the ablated region of the host somite using a microscalpel. In some cases, donor fragments were injected with fluorescent dyes prior to excision to allow the orientation of transplanted fragments to be determined at the time of surgery and to monitor the production of myofibers after transplantation. Eggs were then sealed with Parafilm and re-incubated for 24-48 hours. Details of the DML transplantation surgeries and their outcomes are given in Table 2.

Fluorescent dye injection

Fluorescent lipophilic dye injection was used to evaluate myofiber production from operated somites and to monitor transplanted tissue fragment orientation. Embryos were iontophoretically micro-injected with a 0.2% (weight/volume) concentration of 1,1′, di-octadecyl-3,3,3′,3′,-tetramethylindo-carbocyanine perchlorate (DiI) or with 3, 3′-dioctadecyloxacarbocyanine perchlorate (DiO) solution dissolved in glycofurol (Sigma) and dye-labeling was recorded by fluorescence microphotometry as described previously (Denetclaw et al., 1997; Denetclaw and Ordahl, 2000).

Tissue preparation for antibody labeling and confocal microscopy

To assess the degree of somitic myogenesis in embryos having undergone ablations and in quail-chick chimeras, antibodies to quail (QCPN) and to muscle-specific proteins (desmin or myosin) were used in embryo whole mounts. Embryos were harvested, cleaned free of extra-embryonic membranes, fixed overnight at 4°C in 4% paraformaldehyde in PBS, and then blocked and permeablized in PBS containing 1% bovine serum albumin, 1% Triton X-100, and 10% goat serum. This solution, without goat serum, was also used to dilute antibodies to their indicated working concentrations. Embryos were subsequently incubated overnight at 4°C with QCPN anti-quail monoclonal antibody (Developmental Studies Hybridoma Bank), diluted 1:20. After extensive washing with PBS, embryos were incubated with goat anti-mouse Alexa 488-conjugated secondary antibody (Molecular Probes, Inc), diluted 1:250. Embryos were then incubated overnight at 4°C with anti-desmin polyclonal antibody (Sigma), diluted 1:500. Finally after washing in PBS, embryos were again exposed to secondary antibody (goat anti-rabbit Alexa 546 secondary antibody from Molecular probes, Inc.) diluted 1:250. All secondary antibody incubations were for 2 hours in a dark environment and were carried out at room temperature. Embryos labeled with antibodies (and/or injected with fluorescent dyes) were subsequently prepared for confocal microscopy analysis by cutting down the length of the neural tube and making transverse cuts several somites cranial and caudal to the experimentally manipulated somite. The embryo tissue piece was then placed in PBS in a chamber custom made from electrical tape and oriented such that its dorsolateral side was adjacent to the coverslip. Nail polish sealed the coverslip to the slide.

Confocal microscopy and digital image processing

Confocal microscopy was performed using a Nikon E600FN Physioscope attached to a PCM2000 confocal laser scanning unit (Nikon Inc.) and computer controlled by C-imaging™ Simple32 software (Compix Inc.). The confocal laser scanning and imaging procedures have been recently described (Denetclaw and Ordahl, 2000).

Conventional histology

Some chimeric embryos were analysed by Feulgen staining to reveal the quail nucleolus as previously described (Le Douarin, 1973; Ordahl and Le Douarin, 1992) except that embryos were fixed in 4% paraformaldehyde in PBS and embedded in paraffin. Transverse serial sections were cut at 10 μm intervals through the embryo at the axial level of interest and sections were placed on Super Frost slides (Fisher) and dried overnight on a slide warmer. Slides were then processed for the Feulgen stain reaction as described previously (Le Douarin, 1973; Ordahl and Le Douarin, 1992) and viewed using a Zeiss axiophot photomicroscope fitted with a color CCD camera and connected to a computer for digital image capture (see Dockter and Ordahl, 1998).

RESULTS

Ablation of myotomal precursor cells in the somite dorsomedial quadrant (DMQ)

Previous experiments demonstrate that the somite is developmentally plastic when it is first formed (stage I somite, ss I; see Fig. 1A) but that by ss III (an interval of approximately 200 minutes), a sharp compartmentalization of potentiality has occurred (Aoyama and Asamoto, 1988; Dockter and Ordahl, 2000). To determine if the somite can compensate for loss of a specific population of myogenic precursor cells we ablated the DMQs of 3 adjacent somites, which contain the precursors to the epaxial myotome (Williams and Ordahl, 1997). After 2 days of re-incubation, anti-myosin antibody staining showed that the segmented muscle pattern was absent in the medial-most (epaxial) regions of the targeted somites (Fig. 3A). The laterally located muscle tissue in the operated somites may represent hypaxial muscle but, as the cranial two somites are fore-limb-level, could also include epaxial myocytes cells that had already been 'born' prior to the time of ablation. The latter conclusion is supported by two observations. First, the three DMQs were ablated in somites at ss IX, X and XI; 3-6 hours after the first epaxial myotomal myocytes have been shown to be born (ss VII) in wing-level somites (Kaehn et al., 1988). Second, the earliest-born epaxial myotomal myocytes have been shown to occupy the lateral-most position in the myotome (Denetclaw et al., 1997). To test this conclusion further, wing-level DMQs were ablated at ss III and ss VI followed by

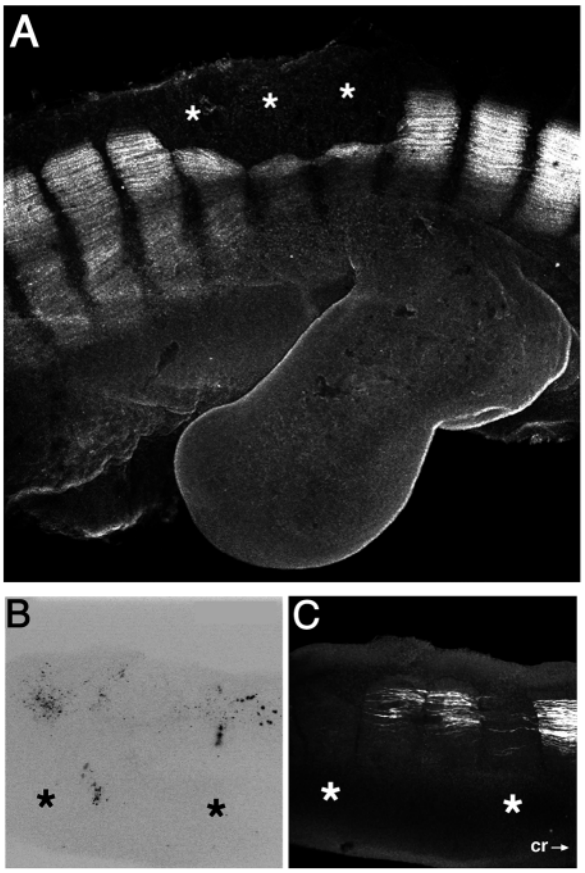

Fig. 3. Ablation of somite dorsomedial quadrant blocks epaxial myotome formation. (A) Fluorescent myosin antibody staining image of a 4-day chick embryo in which the dorsomedial quadrants (DMQs) of three adjacent somites (ss IX-XI) were ablated 2 days earlier. The medial portion of the myotome is missing in all three operated somites (asterisks). (B,C) Confocal images of somites of a day-3 embryo after DMQs were ablated in ss III and ss VI somites the previous day and DiI-injected into the dorsal cut edge of the somite epithelium. (B) DiI-labeled dermomyotome cells (black spots) are evident but no labeled myotome fibers appear in either operated somite (asterisks). In this panel the gray-scale image is inverted to provide better contrast (as described in Denetclaw et al., 1997). (C) Anti-myosin antibody staining shows myotome fibers present in unoperated somites, but no myotome fibers in the somite that was operated at ss III and few fibers in that operated at ss VI. Cr→, designates the cranial direction. B and C are at the same magnification.

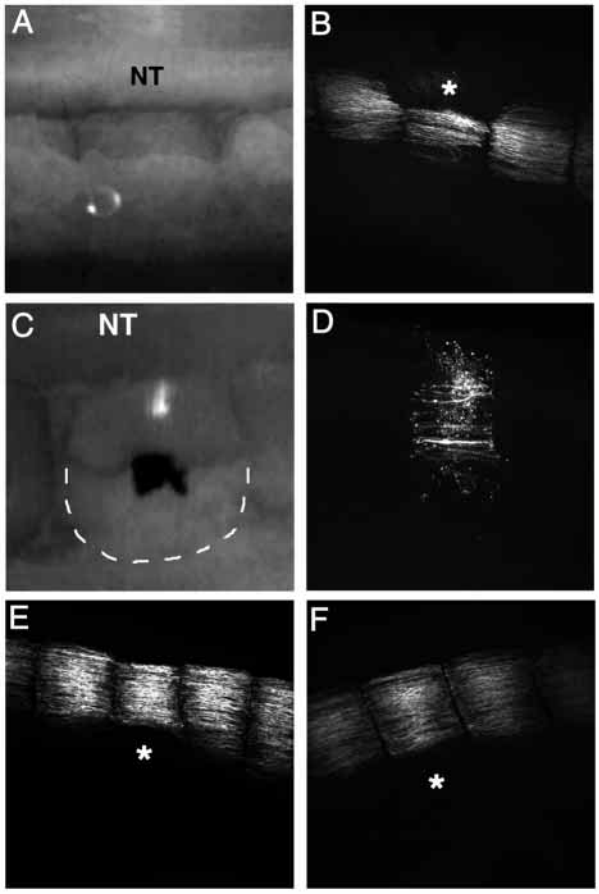

Fig. 4. Ablation of dermomyotome regions. (A,B) Ablation of the DML. (A) After incising and retracting the superficial ectoderm, the dermomyotome DML was ablated. (B) After overnight incubation, confocal imaging using myosin antibody labeling showed that the myotome of the operated somite (asterisk) is truncated medially indicating interrupted myotome growth. (C-E) Ablation of the dermomyotome lateral to the DML. (C) The cut edge of the DML is almost discernable immediately medial to the more prominent cut edge of the ectoderm epithelium. The lateral region of the dermomyotome was ablated (outlined by dashed line) leaving the DML intact. The tilt of the embryo in this image foreshortens the ablated region. After ablation, DiI was injected into the DML (white spot) and a carbon particle implanted into the ablated region (black area). (D) After overnight incubation, confocal imaging of DiI indicates that the injected site gave rise to myotome fibers that were widely distributed along the mediolateral axis of the somite. (E) Confocal imaging of myosin antibody staining in the operated somite (asterisk) shows that myotome development was comparable to that of neighboring, unoperated somites. (F) Confocal imaging of myosin staining in a somite (asterisk) in which a craniocaudal incision was made between the DML and the lateral portion of the dermomyotome the previous day. The myotome of this somite grew to a similar extent to that of neighboring, unoperated somites. NT, neural tube.

injection of fluorescent DiI into the cut free edge of the remaining dorsal epithelium, a likely site from which compensatory muscle precursor cells might arise. After overnight re-incubation, no dye-labeled myotome fibers could be detected (Fig. 3B), indicating that compensatory myotome fibers did not arise from the dye-injected sites. Moreover, no myosin-positive labeled fibers were present after ablation of the ss III somite and very few myotome fibers were present in the somite from which the DMQ was ablated at ss VI (Fig. 3C). In this latter case, the few myofibers observed may have crossed over from adjacent somites but we cannot rule out the possibility that they arose from the operated somite prior to the time of ablation. Therefore ablation of epaxial myotome precursor cells well-prior to the onset of myotome formation (ss III) results in a complete absence of the epaxial myotome, while ablation closer to the time of onset (ss VI) removes the vast majority of, if not all, epaxial myotome precursor cells. Taken together, these results demonstrate that, once ablated in ss III or older somites, ‘replacement’ epaxial myotome precursor cells can neither be regenerated nor recruited from other regions of the somite.

Focal location of myotomal precursor cells in the DML of the dermomyotome

Dye injection lineage tracing indicates that the direct precursors to myotomal myocytes are concentrated along the DML and a portion of the cranial lip of the ssVIII dermomyotome epithelium (Denetclaw et al., 1997; see Fig. 1E). Ablation of the DML of an ss X wing level somite (Fig. 4A) resulted in loss of the medial portion of the epaxial myotome the next day (Fig. 4B; Table 1) indicating that further epaxial myotomal growth was blocked by the surgery. The complementary experiment, in which the DML was left in place but the entire dermomyotome lateral to the DML ablated (Fig. 4C), resulted in formation of myotome by the next day that was indistinguishable from its neighbors (Fig. 4E). Dye-labeling of the DML at the time of surgery (Fig. 4C) resulted in a large number of DiI-labeled myotome fibers dispersed throughout much of the medial-to-lateral extent of the myotome (Fig. 4D) confirming that the formed muscle in that segment indeed derived from the DML and not from another source. Finally, a control experiment in which a surgical incision separated the DML from the rest of the dermomyotome, caused no defect in myotome formation (Fig. 4F). Thus surgery, per se, neither activates nor suppresses potentially or fully active precursor cells in non-DML regions of the dermomyotome. Taken together, the results outlined above and in Table 1 demonstrate that once myotome formation has begun, the DML contains sufficient numbers of precursor cells to generate the entire epaxial primary myotome and that contributory cells from other regions of the somite are not necessary. We interpret DML ablation results presented elsewhere (see fig. 6 in Kahane et al., 1998a) as showing a similar cessation in dorsomedial-ward expansion of the primary myotome.

Table 1. DML and DMQ ablations

Embryo/ exp. #	Ablation type	Somite no.	Somite stage	Hours re-inc.	Myotome devel.
1	DML	30	IX,X,XI	48	truncated
2	Lateral DM	24	VII	20	normal
3	Lateral DM	22	VII	20	normal
4	Lateral DM	26	IX	20	normal
5	Lateral DM	25	VIII	20	normal
6	Lateral DM	27	IX	20	normal
7	Lateral DM	23	VIII	20	normal
8	DML	27	X	20	truncated
9	DML	25	X	20	truncated
10	DML	27	X	20	truncated
11	DML	29	X	20	truncated
12	Mock	26	VII	20	normal
13	DMQ	21	III,VI	20	truncated
14	DMQ	23	III,VI	20	truncated
15	DMQ	21	III,VI	20	truncated
16	DMQ	17	I,III	20	truncated
17	Mock	21	VII	45	normal
18	DML	21	VI	45	truncated
19	DMQ	17	I,III	45	normal
20	DML	30	XIII	20	truncated
21	DML	26	IX	20	truncated
22	DML	27	X	20	truncated
23	DML	28	XII	20	normal
24	DML	31	XII	20	truncated
25	DML	26	IX	20	truncated
26	DML	25	IX	20	truncated
27	Mock	24	IX	20	normal
28	DMQ	14	IV	20	truncated
29	DML	32	XIV	20	truncated
30	DML	18	XIV	20	truncated
31	DML	26	VII	20	truncated
32	DML	20	VII	20	truncated
33	DML	25	IX	20	truncated

Recorded laboratory notes for DML ablation #23 indicate that some DMQ remained adherent to the neural tube and, although not recorded, a similar adhesion may explain the result in DMQ ablation #19 which was among the first ablations performed in this series. Somite number (Somite no.) reflects the total number of formed somites in the embryo, a sensitive index of embryo age. Somite stage indicates developmental age of the targeted somites in each experiment.

Transplantation of the DML from quail somites into chick somites (q→c chimeras)

If the somite DML is both necessary and sufficient to generate the epaxial myotome then it should be possible to restore myotome growth and morphogenesis in a somite with an ablated DML by transplantation of a new DML from another somite. To test this hypothesis, the DML of individual wing-level somites (between ss VIII and ss XI) were ablated in ED2 chick host embryos in the same manner as described above.

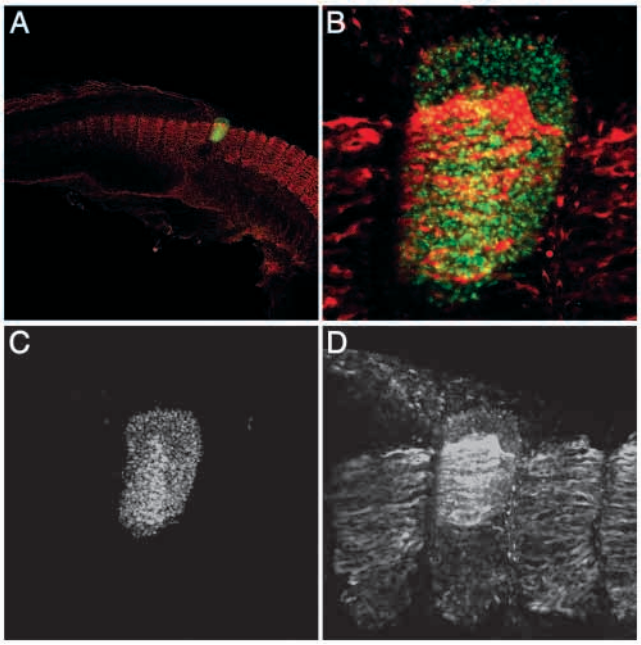

Fig. 5. Replacement of chick DML with that of quail; confocal analysis. (A) Low power confocal image of desmin antibody staining (red) and QCPN anti-quail antibody staining (green) of a chick embryo in which the DML of a single somite was replaced by that of quail the previous day. (B) Higher magnification of the recombinant somite shown in A. Note that the medial extent of myotome (red) is comparable to that of neighboring, unoperated somites (see also A). The quail DML extending medialward beyond the myotome is visible owing to the anti-quail antibody staining of its nuclei. (C) Grey-scale image of anti-quail staining of the same somite showing that the quail DML generated cells in both the dermomyotome and myotome. Myotome cell nuclei can be distinguished by their characteristic concentration in the central region of the segment. (D) Grey-scale image of anti-desmin staining of the same somite. Note that the quail DML has a higher background staining with this antibody than the chick. Apparent staining mediocaudal to the operated somite is a background artifact.

Each excised DML was then replaced with that of a Japanese quail embryo somite at an equivalent stage of development (q→c chimeras; Table 2). The Japanese quail was used as a source of donor DMLs because the progeny derived from the grafted quail donor tissue can be histologically distinguished from the chick host cells.

After overnight reincubation of transplanted embryos, confocal imaging showed that myotome growth in the recombinant somite was indistinguishable from that in the adjacent unoperated somites (Fig. 5A,B). Moreover, the pattern of quail nuclei revealed by QCPN staining showed that the transplanted DML gave rise to both dermomyotome and myotome nuclei (see legend, Fig. 5C), a result consistent with the dye-injection lineage analysis of the DML (Denetclaw et al., 1997). Finally, desmin antibody labeling shows that the extent of medial-ward growth of the chimeric myotome was comparable to that within the adjacent, unoperated host somites (Fig. 5D).

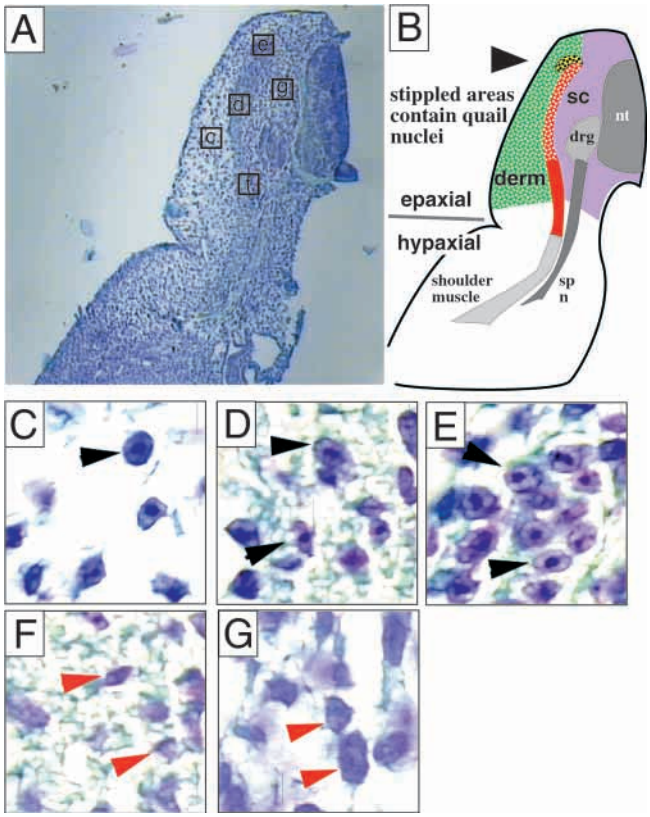

Fig. 6. Histological analysis of recombinant somite bearing quail DML. (A) Transverse section through a recombinant somite bearing a quail DML 2 days after transplantation and stained with Feulgen reagent to distinguish quail and chick nuclei. Boxes marked c-g indicate areas shown at higher magnification in C-G, respectively. (B) Diagrammatic representation of transverse section shown in A indicating areas containing quail nuclei (stippled) and chick nuclei (non-stippled). The DML (yellow) is all that is left of the dermomyotome because the major portion of this epithelium has already become dermatome mesenchyme (green; derm) by the time of harvest. Myotome is shown in red and sclerotome (sc) in violet. The dorsal root ganglion (drg), neural tube (nt), spinal nerve (sp n) and shoulder (hypaxial) muscles are indicated in grey. (C-E) High magnification views of the following regions in which only quail nuclei (black arrowheads) are seen: (C) dermatome; (D) dorsomedial region of epaxial myotome; (E) DML; (F,G) high magnification views of regions comprising only chick nuclei (red arrowheads); (F) ventrolateral region of epaxial myotome; (G) sclerotome.

Three such chimeric embryos, after reincubation for 2 days, were embedded in paraffin, sectioned transversely and stained using the Feulgen reaction to distinguish the quail and chick nuclei (Fig. 6A) and their distribution in different tissues to be analyzed in detail (summarized in Fig. 6B). In each of these embryos, the DML and the dorsomedial-most extent of the epaxial myotome comprised exclusively quail cells, which contain the distinctive nucleolar marker (Fig. 6D,E). By contrast, the ventrolateral-most region of the epaxial myotome and the entire hypaxial musculature comprised chick host cells, which lack the nucleolar marker (Fig. 6F). The absence of quail cells from hypaxial muscle is expected because the precursors to these muscles have been previously shown to be located in the lateral half of wing-level somites (Ordahl and Le Douarin, 1992) specifically within the somite dorsolateral quadrant (Williams and Ordahl, 2000). The ventrolateral location of chick cells in the epaxial myotome is consistent with the DML of the target chick somite having already produced some myotomal daughter cells prior to the time of its ablation. The transition boundary between the chick and quail regions of the myotome is sharp and the uniform density of quail cell composition within the major, dorsomedial portion of the epaxial myotome establishes that the donor DML re-established both the quantitative and patterning aspects of myotome growth. In these embryos the bulk of the dermomyotome has already de-epithelialized and the mesenchymal dermatome is composed of quail cells (Fig. 6C). This finding is consistent with the generation of dermomyotome by the DML (see Fig. 5) and demonstrates that the DML generates epaxial dermal precursor cells in addition to the precursors of the epaxial myotome. The sclerotome, by contrast, was found to be free of quail cells (Fig. 6G), even in its most dorsal extent, indicating that cells from the somite DML do not contribute to sclerotome mesenchyme in any region of the somite during the 48-hour incubation period used in these studies. The absence of donor cells in sclerotome is consistent with previous studies from this laboratory of the developmental potential of the dermomyotome and sclerotome (Williams and Ordahl, 1997; Dockter and Ordahl, 1998; Dockter and Ordahl, 2000; Williams and Ordahl, 2000). Finally, these results are consistent with outcome #1 in Fig. 2B.

Transplantation of the DML from chick somites into quail somites (c→q chimeras)

In the experiments above, continued myotome growth after transplantation was attributed solely to the quail DML because the newly formed myotome appeared to comprise exclusively myofibers containing quail nuclei. Might a small contribution of chick myotome cells in the new growth region of the myotome have gone undetected? The presence of a small number of such chick myotome fibers within the 'quail domain' of the chimeric myotome would be consistent with the 'pioneer' fiber hypothesis (Kahane et al., 1998b) (Figs 1F and 2B, outcome #2). This is an important consideration because, using the Feulgen staining method it is difficult to detect the rare chick nucleus within a preponderance of quail nuclei.

To determine if a small number of non-DML-derived cells

might contribute to new primary myotome growth, we performed the reverse experiment; transplantation of a chick DML into a quail embryo (c→q chimera). Using this approach quantitative detection of individual, isolated quail myofiber nuclei within a myotome comprising chiefly chick myotome fibers is feasible, through the use of the anti-quail antibody (QCPN) fluorescently labeled and detected by confocal microscopy. Eleven c→q DML chimeras were prepared in a

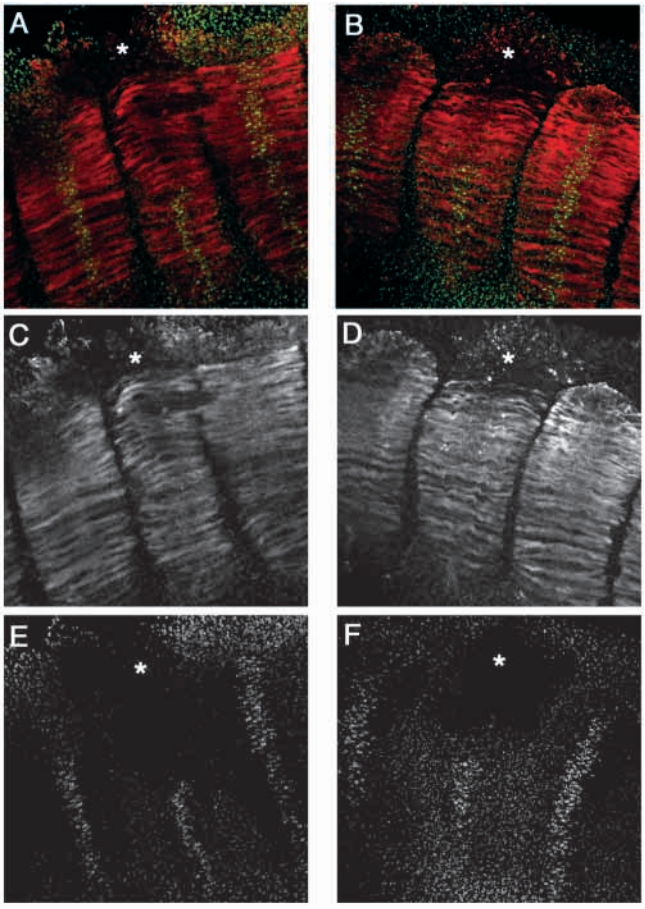

Fig. 7. Older myotome cells absent in new myotome growth zone after DML replacement. False color panels of two transplant examples (A,C,E) and (B,D,F) showing no quail myotome fibers in the chick myotome domain following chick-to-quail DML transplantation. (A,B) Desmin-labeled myotome fibers in recombinant and quail host somites are red and QCPN labeled quail nuclei are green. Long trails of centrally located quail nuclei (green) characterize the host-derived quail myotome fibers, whereas, in recombinant somites, the quail nuclear trail ends abruptly due to the presence of only chick-derived myotome fibers. (C,D) Recombinant and host somites labeled with desmin antibody show that myotome fibers are similar in appearance and have a similar ability to expand in a dorsomedial-ward direction. (E,F) Quail nuclear labeling using the QCPN antibody shows that host somites show long, progressive trails of central nuclei in the myotome. In contrast, this nuclear labeling appearance is halted in the area occupied by the chick-derived myotome fibers. Similarly, the dermomyotome overlying the new myotome domain is also free of quail nuclei. The asterisk marking recombinant somites is placed in the translocation/elongation zone in the recombinant chick domain where myocytes are in active elongation but not yet fully expanded as unit-length myotome fibers (see Fig. 1).

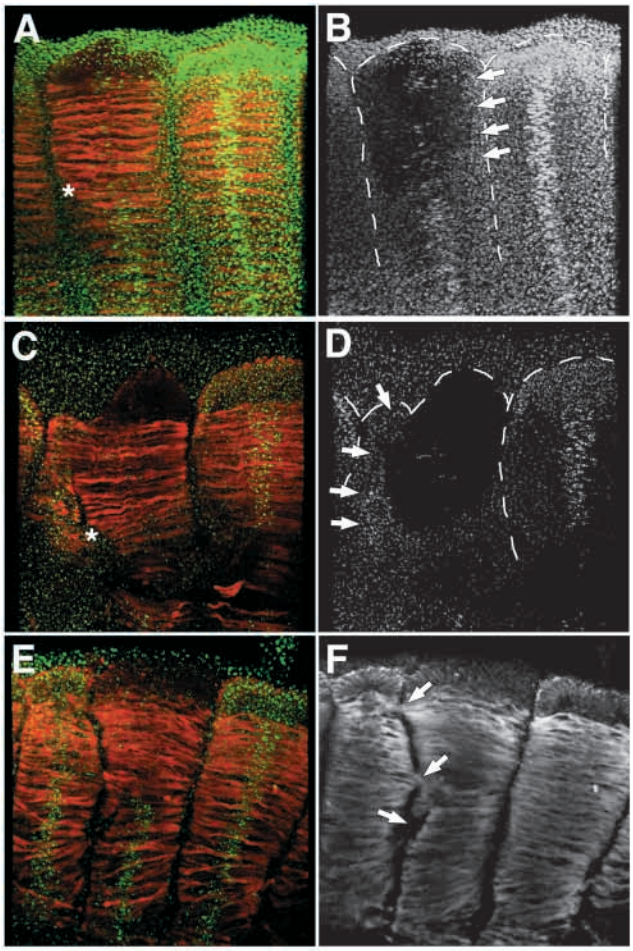

Fig. 8. Examples of myotome fibers with quail nuclei in chick myotome growth regions following chick-to-quail DML transplantation. (A) False color panel of recombinant c→q 11 (Table 2) tilted +24 degrees in the y-axis from its 0 degree position showing 12 centrally positioned quail nuclei in the somite dispersed over the whole mediolateral growth region of the chick DML transplant. The asterisk, marks the boundary of the quail- and chick-derived myotomes. Myotome fibers stained for desmin are red and quail nuclei labeled with QCPN are stained green. (B) Grayscale image of QCPN stained nuclei from A show quail nuclei in the central myotome layer and also in the cranial dermomyotome border (arrows). (C) False color panel of c→q #10 (Table 2) tilted −36 degrees in the y-axis from its 0 degree position showing 10 centrally positioned quail nuclei in the chick myotome. In this case, the quail nuclei were clustered and not distributed over the whole mediolateral extent of the chick-derived myotome. The asterisk, identifies a vertical split showing that the chick DML transplant did not initially integrate into the quail dermomyotome, but did later in the dorsomedial half of the somite. (D) Grayscale image of QCPN stained nuclei from C show quail nuclei limited to the central chick myotome layer and also heavily concentrated at the caudal dermomyotome border (arrows). In both B and D dashed lines outline somite boundaries. (E) False color panel tilted −36 degrees in the y-axis from its 0 degree position showing a few myotome fibers with quail nuclei in the chick-derived myotome. (F) Grayscale image showing desmin-labeled myotome fibers from several deep optical confocal z-sections showing myotome fiber cross-over from an adjacent quail somite into the chick-derived myotome region (arrows).

Table 2. DML transplantation experiments

Embryo	Somite no.	Somite stage	Hours re-inc.	Histology	Implant orientation	Host DM growth	Host nuclei in Donor zone
Q→C 1	H21 dNR	XII XX	45	M/F	positive	NR	none detected
Q→C 2	H27 dNR	X XX	45	M/F	positive	NR	none detected
Q→C 3	H29 dNR	ND XX	45	M/F	NR	NR	none detected
Q→C 4	H22 d35	VII IX	20	Q/D	positive	NR	none detected
Q→C 5	H27 dNR	IX XIV	20	Q/D	positive	NR	none detected
C→Q 1	H24 d23	XIII XI	20	Q/D	NR	no	none detected
C→Q 2	H24 d27	XII XII	20	Q/D	inverted	no	none detected
C→Q 3	H28 d23	XVII XII	20	Q/D	positive	no	none detected
C→Q 4	H25 d24	XIII XII	20	Q/D	positive	cranial	none detected
C→Q 5	H25 d24	XIV XIII	20	Q/D	inverted	no	none detected
C→Q 6	H29 d20	XIV XII	20	Q/D	inverted	no	none detected
C→Q 7	H18 d24	XII XII	20	Q/D	positive	no	none detected
C→Q 8	H25 d20	XII ND	20	Q/D	NR	no	none detected
C→Q 9	H18 d24	XII XIX	20	Q/D	NR	caudal	2
C→Q 10	H26 d21	X XIV	20	Q/D	positive	caudal	10
C→Q 11	H27 d24	XIII XIII	20	Q/D	positive	cranial	12

Abbreviations: C→Q, chick to quail transplant; Q→C, quail to chick transplant; H, host; d, donor; D, desmin immunohistochemistry; M, myosin immunohistochemistry; F, Feulgen staining reaction; NR, not recorded. Other designations as in Table 1.

manner essentially as described above for the q→c DML chimeras except that the use of fluorescence allowed a more detailed control and recording of surgical aspects of the experiment (see Methods and Table 2). The myotome and dermomyotome of somites bearing recombinant DMLs were then analyzed by confocal microscopy essentially as described above, except that detailed scan-by-scan image analysis was made of each recombinant somite to determine if individual quail-derived nuclei were present in the new growth (chick domain) of the myotome.

Fig. 7 shows the confocal analysis of two chick→quail chimeras bearing DML recombinant somites (see c→q #1 and #2; Table 2) after overnight re-incubation. Anti-desmin and QCPN antibody labeling was used to reveal the presence of differentiated myotomal myofibers and quail nuclei (red and green, respectively, in A and B). Both recombinant somites showed robust myotome development that was essentially indistinguishable from that of adjacent unoperated host somites (Fig. 7A-D) despite the fact that the donor DML was implanted in reverse craniocaudal orientation in c→q #2 (see Table 2). Successive confocal laser scans in the z-axis through these two recombinant somites demonstrated that no quail nuclei resided within the chick-derived region of the myotome or overlying dermomyotome (Fig. 7E,F). This organization of the myotome of the chick-DML-recombinant somites is exactly the reverse of that of the quail-DML-recombinants discussed above and diagrammed in Fig. 6B. Of the remaining c→q chimeras, six (Table 2, #3-8) gave results identical to those illustrated for c→q #1 and 2. Thus, in chimeras #1-8, epaxial myotome and dermomyotome expansion was driven exclusively by addition of new cells from the transplanted donor DML and did not require or incorporate cells from other regions of the somite and specifically, from lateral (older) regions of the myotome.

Chick→quail DML recombinants giving rise to myotome fibers intermingled from both species

Of eleven chimeras (#9-11; Table 2), a small number of quail nuclei were detected in the chick-derived region of three c→q recombinant myotomes. Confocal analysis (Fig. 8) demonstrated that, in the two of these instances that gave the most quail myofibers (c→q #10 and 11, Table 2), host quail dermomyotome cells participated with the transplanted chick cells in DML activity. This is evident from the presence of quail nuclei respectively within the cranial or caudal border of the dermomyotome of the chimeric somite (see arrows, Fig. 8B,D) that were generated concommitant with the generation of the quail myofibers. Interestingly, co-incorporation of host cells into the cranial lip also occurred in another instance (c→q

#4, Table 2) but no quail nuclei were found in the chick myotome zone in that case. Finally, in the third case in which quail nuclei were found in the chick region of the myotome (c→q #9), detailed confocal analysis showed that myofiber(s) from the adjacent host somite extended cranially into the chick domain of the recombinant somite myotome (Fig. 8E,F). We conclude, therefore, that the presence of a small number of quail myocyte nuclei within the chick domain of these three recombinant somites is due to surgical artifact rather than the translocation or displacement of myotome fibers from more lateral (older) regions of the myotome.

DISCUSSION

The DML is the source of new cells for growth of the primary myotome and dermomyotome epithelium

The ablation experiments reported here demonstrate that the DML of the somite dermomyotome epithelium is necessary for myotome growth and morphogenesis. Ablation of the DML blocks further myotome growth. Conversely, after ablation of the entire dermomyotome except for the DML, myotome growth is unaffected. Transplantation experiments show that a donor DML serves as the source of new myocytes that enter the myotome layer asymmetrically along the dorsomedial boundary of the myotome. Taken together, these results indicate that the DML continuously emits two streams of cells (see Fig. 9). One stream translocates to the subjacent myotome layer along its dorsomedial boundary and these cells subsequently elongate and differentiate into myotome fibers. A second stream simultaneously enters the dermomyotome epithelium. We conclude, that the somite DML is both necessary and sufficient to drive the growth and morphogenesis of both the myotome as well as the overlying dermomyotome epithelium.

The expansion of the primary epaxial myotome and dermomytome along the somite mediolateral axis (i.e. in a ventrolateral-to-dorsomedial direction) can be attributed to (see Fig. 9; and Denetclaw et al., 1997; Denetclaw and Ordahl, 2000 and Denetclaw et al., 2001): (i) addition of new cells asymmetrically along the dorsomedial margin of the myotome; (ii) convergent extension as those cells elongate; (iii) hypertrophy of myotome fibers that accompanies differentiation and maturation; and (iv) asymmetric addition of

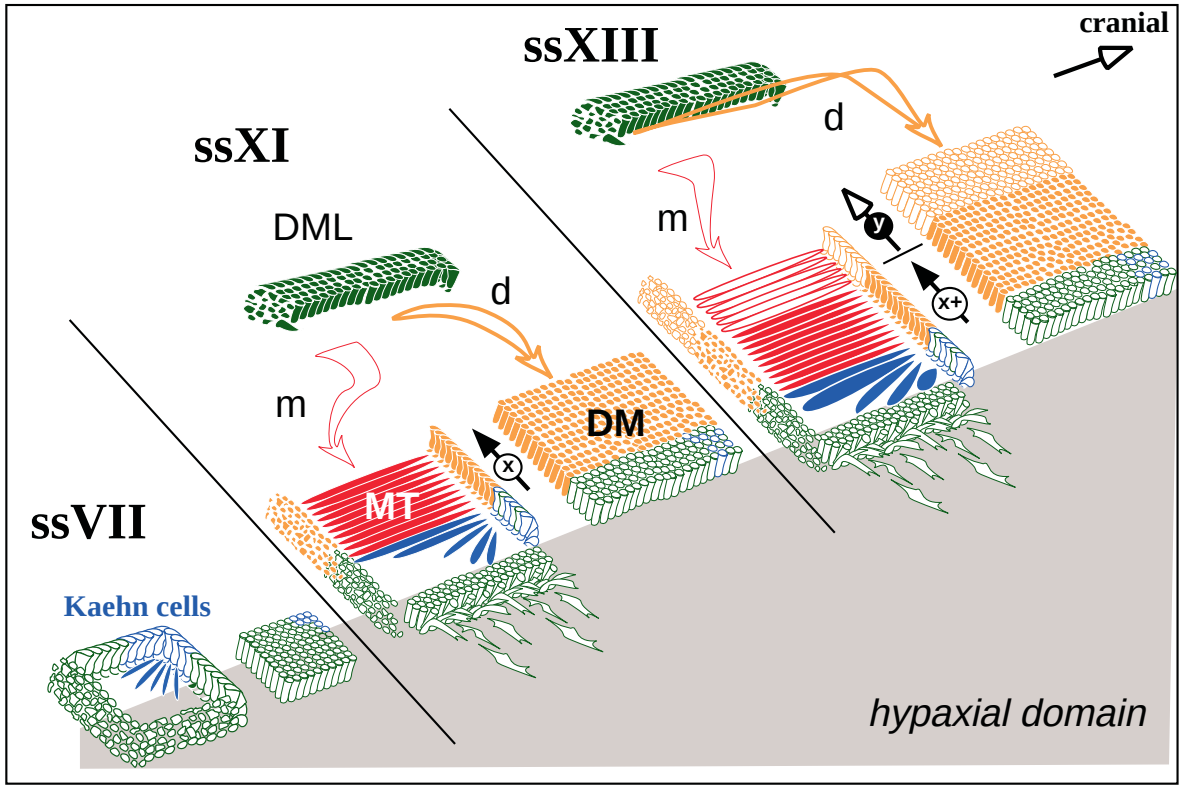

Fig. 9. DML-directed growth and morphogenesis of the epaxial primary myotome and dermomyotome. After initiation of development at somite stage VII, new myotome and dermomyotome cells generated by the DML are displaced laterally as an intermingled stream of cells fated to enter either the myotome or dermomyotome (DML shown in dark green at ss XI and XIII). DML-dependent growth occurs through the asymmetric addition of new cells to the medial-most margin of the myotome (m) and dermomyotome (d) resulting in the DML being displaced medially. The net growth increment of the somite between ss VII and XI is indicated by the arrow marked ‘x’. Note that Kaehn cells (the oldest myotome cells in each segment), as well as some dermomyotome cells that were at the original site of birth of the Kaehn cells (dark blue), are progressively displaced laterally as the somite grows. During the interval between ss XI and XIII, that process continues (growth increment ‘y’) but maturing myocytes in the lateral region of the myotome undergo hypertophy further expanding the myotome and, possibly and to an unknown extent, through secondary addition of new myocytes intercalated from the cranial or caudal dermomytome lips and/or other sources (x+). The dermomyotome continues to expand through hyperplasia. In fore-limb-level somites, cells in the region of the dermomyotome migrate into the hypaxial domain where they form blood vessels and limb muscles.

new dermomyotome epithelial cells between the DML and the sheet region of the dermomyotome (d) and the subsequent mitotic expansion of those cells after leaving the DML. The possibility that some cells displaced from the DML into the myotome layer might remain quiescent for a period before giving rise to myotome fibers remains untested.

The results and conclusions outlined above are consistent with earlier studies (Holtzer and Detwiler, 1953), in which an ablation of the greater portion of amphibian somites was shown to block dorsal (epaxial) muscle formation when made medially rather than laterally, as well as with recent experiments showing that the medial third of the avian dermomyotome is sufficient to give rise to the entire epaxial myotome in each somite segment (Huang and Christ, 2000). However, the results of the experiments reported here are not compatible with a recently proposed model for myotome development that postulates that the primary myotome consists of a small group of post-mitotic 'pioneer' cells localized along the cranial lip of the dermomyotome and which extend as myofibers to the caudal dermomyotome lip very early during somitogenesis (Kahane et al., 1998b; Kahane et al., 1998a; Cinnamon et al., 1999). In this model, further dorsomedial expansion of the myotome results from intercalation events, originating symmetrically along both the cranial and caudal demomyotome lips, which displace the primary fibers more-or-less equidistantly throughout the myotome (Kahane et al., 1998b; Kahane et al., 1998a; Cinnamon et al., 1999; illustrated in Fig. 1F). Lateral dermomyotome ablation, such as that shown in Fig. 3, would be expected to substantially or completely block further mediolateral expansion of the myotome in that model as well as in that proposed by Kaehn et al. (Kaehn et al., 1988; illustrated in Fig. 1D). In addition, because pre-existing myotome fibers were quantitatively excluded from the new myotome growth zone in recombinant somites, we conclude that 'pioneer cells' such as those proposed by Kalcheim and coworkers (Kahane et al., 1998b; Kahane et al., 1998a; Cinnamon et al., 1999; see Figs 1F and 2B) are neither necessary for nor present within new myotome growth.

In insect embryos, a distinct specified lineage of 'muscle pioneer cells' is proposed to establish the initial somatic muscle pattern and then recruit, pattern and induce other, unspecified cells to participate in myogenesis (Ho et al., 1983; reviewed by Kaehn et al., 1988; Kahane et al., 1998b). Similarly, in zebrafish embryos, 'adaxial cells' represent an early class of muscle cells that establish the epaxial-hypaxial boundary and then migrate to superficial locations to form a specialized class of slow muscle fibers (Devoto et al., 1996; reviewed by Kahane et al., 1998b; Kahane et al., 1998a). In each of these cases, early muscle cells perform what might be termed a 'scaffold' function by providing patterning information for the development of subsequent muscle tissues at later stages.

Scaffolding functions are an important principle in embryonic development and have been described for the development of many tissues and organs (reviewed by Caplan et al., 1983). We proposed that DML-directed growth and morphogenesis of the primary myotome provides such a scaffold function by driving the dorsomedial to ventrolateral vector of growth of the epaxial domain in each somitic segment (Denetclaw et al., 1997). Because development of other tissues, such as the sclerotomal pre-vertebrae, are controlled by extrinsic influences within the epaxial domain, the scaffolding potential for the primary epaxial myotome may extend to many other tissues in addition to skeletal muscle. Similarly, in the hypaxial domain, the ventrolateral lip of the dermomyotome drives hypaxial myotome development into the body wall in a manner similar to, but in inverted direction to, that of the epaxial myotome (Denetclaw and Ordahl, 2000).

The distal portion of the rib is absent in mice bearing homozygous mutation in the *myf5* gene (Braun et al., 1992). The precursors of this rib segment have recently been shown to reside in the lateral half of the presegmented mesoderm and somite where the somitic precursors of the hypaxial domain of the body also reside (Olivera-Martinez et al., 2000; Ordahl et al., 2000). The present work demonstrates that the DML also drives medial-to-lateral growth of the dermomyotome, and therefore the underlying patterning of the dermis of the skin of the back, which has also been demonstrated to be derived from the medial half of the pre-segmented mesoderm (Olivera-Martinez et al., 2000).

The overall size of the epaxial domain in the early embryo could therefore be established by the combination of the lateral-to-medial growth vector of the DML, in concert with the ventral-to-dorsal growth vector generated by the neural tube. The growth vector(s) of the sclerotome is unknown but may be important for space-filling between the myotome and neural tube because early sclerotome cells carry limited amounts of determined morphogenetic information (Dockter and Ordahl, 1998; Nowicki and Burke, 2000). The uni-segmental patterning of the primary myotome also establishes the muscular connections between nascent vertebrae (Brand-Saberi and Christ, 2000). Finally, although the source of cells and mechanisms for the secondary stage of myotome formation are not yet well understood (see Fig. 1C) the fact that this occurs directly beneath and in close apposition to the primary myotome suggest that the latter also provides a scaffold for its formation. We hypothesize, therefore, even though primary myotome formation in avian embryos may be mechanistically different from early muscle formation in other vertebrates and insects, that the primary myotome and the overlying dermomytome provide a developmental scaffolding function that is fundamentally important not only for later muscle development but also for the overall patterning of the embryonic body.

Contribution of cells from the cranial and caudal lips of the dermomyotome epithelium

The first skeletal muscle cells to differentiate, Kaehn cells (Fig. 9), are born in the craniomedial corner of the somite (Kaehn et al., 1988; see Fig. 1B) and correspond to the cells dubbed pioneer cells by Kalcheim and coworkers (Kahane et al., 1998b; Kahane et al., 1998a; Cinnamon et al., 1999). These cells may constitute a special class, but their postmitotic status and small numbers are not consistent with the tissue mass of the entire primary myotome. As shown here, one important source of additional cellular mass is the DML. Nevertheless, as reported first by Kahane et al. (Kahane et al., 1998a) and by us (Denetclaw and Ordahl, 2000), new myotome cells may also be subsequently added from the cranial and caudal lips of the dermomyotome. The contribution of such cells to the lateral-to-medial growth of the primary myotome depends upon the

degree to which they intercalate between existing fibers that were deposited directly from the DML. Although the contribution of such intercalation has not been quantified it is known that at least some of these cells contribute to superficial-to-deep expansion of the secondary myotome (Kahane et al, 1999; Denetclaw and Ordahl, 2000) (see Fig. 1C) and therefore would be expected to contribute to lateral-to-medial expansion only secondarily, i.e. through myofiber hypertrophy.

More important from the point of view of this work, however, is the conclusion that the cells resident in the caudal and cranial lips of the dermomyotome are products of DML activity. Therefore, generation of new myofibers by such cells must lag behind the medial-ward expansion of the DML. Assuming, for example, that a newly born cranial lip cell must undergo at least one cell cycle prior to generating its first myogenic daughter the lag could encompass several somite stages and thus be well behind the leading edge of DML growth which can be measured easily in terms of somite stages (Denetclaw et al., 1997; Denetclaw and Ordahl, 2000). We conclude, therefore, that DML-directed primary myotome growth precedes that derived from DML-derived cell populations, such as those arrayed along the cranial and caudal lips of the dermomyotome.

Quantitative aspects of DML-dependent growth and morphogenesis

Cells entered the myotome and dermomyotome in recombinant somites bearing a transplanted DML at the same rate as in unoperated host somites because the medial-to-lateral dimension of the myotomes and dermomytomes was equivalent in both (see Figs 4E, 5A,B,D, 8C,D). Previous morphometric analysis of dye injection experiments demonstrated that myotome maturation is greatest along the somite mediolateral axis (Denetclaw et al., 1997; Denetclaw and Ordahl, 2000). Therefore, the surgical interventions described here did not significantly interfere with the rate of myotome and dermomytome growth and morphogenesis.

Interestingly, the craniocaudal dimensions of myotome and dermomyotome generated in DML recombinants were more variable. While in some cases the craniocaudal width of the donor-derived myotome was comparable to that of adjacent host somites (Fig. 7B,D), in other recombinant somites it was narrower (Fig. 7A,C) and in others wider (data not shown). Because myotomes at different axial levels differ in their craniocaudal dimension, it is possible that in some instances this difference could be due to inherent axial-level-specific differences in myocyte elongation rate. In other cases, however, it is possible that deformations of the DML during surgery resulted in the donor DML not fully spanning the craniocaudal dimension of the host DML ablation site. Morphometric analysis implicates such surgical artifacts in the recruitment of host cells into donor regions of the myotome generated by transplanted DMLs (see Fig. 8).

Extrinsic influences on DML activity

The results outlined above indicate that the DML alone has the ability to generate cells for the myotome and dermomytome and may have other intrinsic properties, such as formation of myocytes that are mononuclear (Holtzer et al., 1957; Williams and Ordahl, 1997) or, as noted above, possibly elongate in the craniocaudal dimension to a pre-determined length. In other respects, however, it can be concluded that the DML and its activity is governed by outside influences from surrounding structures and tissues. For example, in each DML transplantation experiment, the direction of myotome growth was medial-to-lateral (a conclusion confirmed by dye-labeling of DMLs prior to transplantation in several cases; data not shown), fiber elongation was restricted to one somite segment and myotome was formed subjacent to dermomyotome. That such properties were governed by extrinsic rather than strictly intrinsic influences is evident from the myotome and dermomyotome formed in chick→quail chimera #2 in which the craniocaudal orientation of the implanted DML was inverted (see Table 2). Despite the fact that such an inversion necessarily changed one other axis of symmetry (either mediolateral or dorsoventral) the resulting myotome resided beneath the dermomyotome and grew in a medial-ward direction. In this and several other cases (see Table 2), the implanted DML correctly re-interpreted the surroundings and grew in correct morphogenetic fashion and in concert with neighboring tissues. Many tissues are known to emit signals that affect somite development (reviewed by Borycki and Emerson, 2000) and we hypothesize, therefore, that the DML is an important target of those signals that govern myotome and dermomyotome development.

Comparison of this model to myotome development in non-avian systems

The impairment and delays in myotome development in mice bearing deletions and/or markers in genes encoding factors involved in myogenic determination may be usefully interpreted in context of the model of myotome growth and morphogenesis developed here for avian systems. For example, several years ago, Buckingham and coworkers showed β-galactosidase staining in the DML of mouse embryos bearing a *lacZ* transgene in one *myf5* locus (Tajbakhsh et al., 1996a). Animals lacking functional Myf5 expression exhibit delayed epaxial muscle development (Braun et al., 1994; Tajbakhsh et al., 1996b; Kablar et al., 1997) despite the delamination of myotomal precursors to the translocation/elongation zone of the myotome (depicted in Fig. 9; Tajbakhsh et al., 1996b; Tajbakhsh et al., 1997). This suggests that early translocation events may be unaffected by the *myf5* mutation whereas elongation and other downstream differentiation processes clearly are. It remains to be seen how far upstream the *myf5* mutation may act and how this mutation affects DML activity.

Experiments in avian embryos have implicated Sonic hedgehog (Shh), arising from the notochord and ventral floor plate, in the control of initiation of primary myotome development (Munsterberg et al., 1995; Munsterberg and Lassar, 1995; Pownall et al., 1996; Borycki et al., 1998). Mouse embryos lacking Shh due to genetic mutation fail to sustain the DML and do not express primary myotome markers (Chiang et al., 1996; Borycki et al., 1999) consistent with the generative power of the DML as proposed here. The importance of the dorsal axial structures in early muscle specification has also been well documented through experimental embryology using avian embryos. A similar role in mouse development has been described through analysis of the mouse embryos bearing the *open brain (opb)* mutation (Sporle et al., 1996) showing that axial levels exhibiting abnormal dorsal neural tube development correlate with areas of defective dermamyotome and primary

myotome formation. Unlike the *myf5* null embryos where the epaxial musculature appears to be rescued by later MyoD expression, in *opb* mutants the epaxial musculature remains undeveloped. Both mice have disrupted Pax3 expression in the dorsomedial dermamyotome (Sporle et al., 1996; Tajbakhsh et al., 1997) consistent with the phenotype of *splotch* mice (Epstein et al., 1991; Goulding et al., 1993; Bober et al., 1994) where neural tube defects can correlate with areas of reduced axial musculature. Such molecular/genetic phenotypes in epaxial muscle development are consistent with intrinsic defects in DML activity and/or extrinsic control of the DML and its ability to productively generate myotome and dermomyotome cells.

Morphological analysis of myotome development in the mouse based on expression of muscle-specific proteins (Venters et al., 1999) described a continuing dorsomedial source of presumptive myotomal cells throughout the period of primary myotome formation as shown here for the chick embryo. The primary myotome was reported as comprising a single population of myocytes differentiating through a MyoD-independent pathway in accord with murine gene expression and *myf5* knock-out and analyses (Buckingham et al., 1992; Tajbakhsh et al., 1996b). In contrast to the direct translocation of cells from their site of origin within the DML to the myotome layer as reported for the chick from this laboratory (Denetclaw et al., 1997; Denetclaw and Ordahl, 2000), in the mouse, myogenic cells were reported as entering the myotome from rostral and caudal dermomyotome lips rather than directly from the DML. Whether the differences reported in mode of entry of presumptive myotomal cells to the myotome are mechanistic differences in chick and mouse development or result from differences in techniques and denotation of stages of epaxial myogenesis remains unresolved by the data reported here. It is possible, however, that differences in the timing of entry and/or differentiation of second-wave myogenic cells into the primary myotome field could account for observed differences between these models.

The DML as an engine of cellular growth and morphogenesis

Quail-chick transplantation has shown that the epaxial dermis is derived from the dermomyotome epithelium (Mauger, 1972; Olivera-Martinez et al., 2000). After DML transplantation at ED2, the epaxial dermomyotome is donor-derived by ED3 (Figs 4, 7, 8) and that by ED4, those donor-derived dermomyotome cells can be chased into the dermal mesenchyme of the epaxial domain (Fig. 5). Thus, DML activity plays a major role in the growth and morphogenesis of the embryonic epaxial domain by generating the cells that give rise to both the primary myotome and dermis, two tissues with very different patterning. As indicated above, some aspects of primary myotome patterning may be intrinsic to the DML. The extent to which intrinsic aspects of DML activity are responsible for dermal patterning remains to be determined. Although the source of cells for successive waves of epaxial muscle development is not yet fully established (see Introduction), available evidence indicates a continuing role for the epaxial portion of the dermomyotome epithelium. A third tissue of unknown origin is the connective tissue of the epaxial muscle. It is possible, therefore, that both muscle myoblast and muscle fibroblasts co-emerge from the DML as it generates the tissues of the epaxial domain.

The authors would like to thank our many colleagues for useful discussions and Jennifer Agard for helpful suggestions on experiments. We thank Nina Kostanian and Sharon Spencer for excellent technical and administrative support. C. P. O. would especially like to acknowledge the efforts and growth of E. B. on this project, which greatly exceeded his job description. This work was supported by grants to CPO from the National Institutes of Health (AR44483) and from the Muscular Dystrophy Association of America. W. F. D. was partly funded through the San Francisco State University Research Infrastructure in Minority Institutions (RIMI) Program from the National Center for Research Resources, NIH Office of Research on Minority Health (P20 RR11805).

REFERENCES

Aoyama, H. and Asamoto, K. (1988). Determination of somite cells: independence of cell differentiation and morphogenesis. *Development* **104**, 15-28.

Bober, E., Franz, T., Arnold, H.-H., Gruss, P. and Tremblay, P. (1994). Pax-3 is required for the development of limb muscles: a possible role for the migration of dermomyotomal muscle progenitor cells. *Development* **120**, 603-612.

Borycki, A. G., Brunk, B., Tajbakhsh, S., Buckingham, M., Chiang, C. and Emerson, C. P., Jr. (1999). Sonic hedgehog controls epaxial muscle determination through Myf5 activation. *Development* **126**, 4053-4063.

Borycki, A. G. and Emerson, C. P., Jr. (2000). Multiple tissue interactions and signal transduction pathways control somite myogenesis. *Curr. Top. Dev. Biol.* **48**, 165-224.

Borycki, A. G., Mendham, L. and Emerson, C. P., Jr. (1998). Control of somite patterning by Sonic hedgehog and its downstream signal response genes. *Development* **125**, 777-790.

Brand-Saberi, B. and Christ, B. (2000). Evolution and development of distinct cell lineages derived from somites. *Curr. Top. Dev. Biol.* **48**, 1-42.

Braun, T., Bober, E., Rudnicki, M., Jaenisch, R. and Arnold, H.-H. (1994). MyoD expression marks the onset of skeletal myogenesis in *Myf-5* mutant mice. *Development* **120**, 3083-3092.

Braun, T., Rudnicki, M., Arnold, H. and Jaenisch, R. (1992). Targeted inactivation of the muscle regulatory gene Myf-5 results in abnormal rib development and perinatal death. *Cell* **71**, 369-382.

Buckingham, M., Houzelstein, D., Lyons, G., Ontell, M., Ott, M. O. and Sassoon, D. (1992). Expression of muscle genes in the mouse embryo. *Sym. Soc. Exp. Biol.* **46**, 203-217.

Caplan, A. I., Fiszman, M. Y. and Eppenberger, H. M. (1983). Molecular and cell isoforms during development. *Science* **221**, 921-927.

Chevallier, A., Kieny, M. and Mauger, A. (1977). Limb-somite relationship: Origin of the limb musculature. *J. Embryol. Exp. Morph.* **41**, 245-258.

Chiang, C., Litingtung, Y., Lee, E., Young, K. E., Corden, J. L., Westphal, H. and Beachy, P. A. (1996). Cyclopia and defective axial patterning in mice lacking Sonic hedgehog gene function. *Nature* **383**, 407-413.

Christ, B., Jacob, H. and Jacob, M. (1974). Uber den ursprung der flugelmuskulature. *Experientia* **30**, 1446-1448.

Cinnamon, Y., Kahane, N. and Kalcheim, C. (1999). Characterization of the early development of specific hypaxial muscles from the ventrolateral myotome. *Development* **126**, 4305-4315.

Denetclaw, W. F. and Ordahl, C. P. (2000). The growth of the dermomyotome and formation of early myotome lineages in thoracolumbar somites of chicken embryos. *Development* **127**, 893-905.

Denetclaw, W. F., Christ, B. and Ordahl, C. P. (1997). Location and growth of epaxial myotome precursor cells. *Development* **124**, 1601-1610.

Devoto, S. H., Melancon, E., Eisen, J. S. and Westerfield, M. (1996). Identification of separate slow and fast muscle precursor cells in vivo, prior to somite formation. *Development* **122**, 3371-3380.

Dockter, J. and Ordahl, C. P. (2000). Dorsoventral axis determination in the somite: a re-examination. *Development* **127**, 2201-2206.

Dockter, J. L. and Ordahl, C. P. (1998). Determination of sclerotome to the cartilage fate. *Development* **125**, 2113-2124.

Epstein, D. J., Vekemans, M. and Gros, P. (1991). Splotch (Sp2H), a mutation affecting development of the mouse neural tube, shows a deletion within the paired homeodomain of Pax-3. *Cell* **67**, 767-774.

Fischel, A. (1895). Zur entwicklung der ventralen rumpf- und extremitatenmuskulatur der Vogel und Saugetiere. *Morph. Jb.* **23**, 544-561.

Goulding, M., Sterrer, S., Fleming, J., Balling, R., Nadeau, J., Moore, K. J., Brown, S. D., Steel, K. P. and Gruss, P. (1993). Analysis of the Pax-3 gene in the mouse mutant splotch. *Genomics* **17**, 355-363.

Ho, R. K., Ball, E. E. and Goodman, C. S. (1983). Muscle pioneers: large mesodermal cells that erect a scaffold for developing muscles and motoneurones in grasshopper embryos. *Nature* **301**, 66-69.

Holtzer, H. and Detwiler, S. R. (1953). Role of the spinal cord in the induction and structuring of the vertebral column. *Anat. Rec.* **115**, 323 (abstract).

Holtzer, H., Marshall, J. M. and Finck, H. (1957). An analysis of myogenesis by the use of fluorescent antimyosin. *J. Biophys. Biochem. Cytol.* **3**, 705-729.

Huang, R. and Christ, B. (2000). Origin of the epaxial and hypaxial myotome in avian embryos. *Anat. Embryol. (Berl)* **202**, 369-374.

Kablar, B., Krastel, K., Ying, C., Asakura, A., Tapscott, S. J. and Rudnicki, M. A. (1997). MyoD and Myf-5 differentially regulate the development of limb versus trunk skeletal muscle. *Development* **124**, 4729-4738.

Kaehn, K., Jacob, H., Christ, B., Hinrichsen, K. and Poelmann, R. (1988). The onset of myotome formation in the chick. *Anat. Embryol.* **177**, 191-201.

Kahane, N., Cinnamon, Y. and Kalcheim, C. (1998a). The cellular mechanism by which the dermomyotome contributes to the second wave of myotome development. *Development* **125**, 4259-4271.

Kahane, N., Cinnamon, Y. and Kalcheim, C. (1998b). The origin and fate of pioneer myotomal cells in the avian embryo. *Mech. De.v* **74**, 59-73.

Le Douarin, N. (1973). A feulgen-positive nucleolus. *Exp. Cell. Res.* **77**, 459-468.

Mauger, A. (1972). Rôle du mésoderme somitique dans le développement du plumage dorsal chez l'embryon de Poulet. I. Origine, capacités de régulation et détermination du mésoderme plumigène. *J. Embryol. Exp. Morphol.* **28**, 341-341.

Munsterberg, A. E., Kitajewski, J., Bumcrot, D. A., McMahon, A. P. and Lassar, A. B. (1995). Combinatorial signaling by Sonic hedgehog and Wnt family members induces myogenic bHLH gene expression in the somite. *Genes Dev* **9**, 2911-2922.

Munsterberg, A. E. and Lassar, A. B. (1995). Combinatorial signals from the neural tube, floor plate and notochord induce myogenic bHLH gene expression in the somite. *Development* **121**, 651-660.

Nowicki, J. L. and Burke, A., C,. (2000). Hox genes and morphological identity: axial versus lateral patterning in the vertebrate mesoderm. *Development* **127**, 4265-4275.

Olivera-Martinez, I., Coltey, M., Dhouailly, D. and Pourquié, O. (2000). Mediolateral somitic origin of ribs and dermis determined by quail- chick chimeras. *Development* **127**, 4611-4617.

Ordahl, C. and Le Douarin, N. (1992). Two myogenic lineages within the developing somite. *Development* **114**, 339-353.

Ordahl, C. P. and Christ, B. (1997). Avian somite transplantation: a review of basic methods. *Methods Cell Biol.* **52**, 3-27.

Ordahl, C. P., Williams, B. A. and Denetclaw, W. (2000). Determination and morphogenesis in myogenic progenitor cells: an experimental embryological approach. *Curr. Top. Dev. Biol.* **48**, 319-367.

Pownall, M. E., Strunk, K. E. and Emerson, C. P., Jr. (1996). Notochord signals control the transcriptional cascade of myogenic bHLH genes in somites of quail embryos. *Development* **122**, 1475-1488.

Sporle, R., Gunther, T., Struwe, M. and Schughart, K. (1996). Severe defects in the formation of epaxial musculature in open brain (opb) mutant mouse embryos. *Development* **122**, 79-86.

Tajbakhsh, S., Bober, E., Babinet, C., Pournin, S., Arnold, H.-H. and Buckingham, M. (1996a). Gene targeting the *myf-5* locus with *nlacZ* reveals expression of this myogenic factor in mature skeletal muscle fibres as well as early embryonic muscle. *Dev. Dynam.* **206**, 291-300.

Tajbakhsh, S., Rocancourt, D. and Buckingham, M. (1996b). Muscle progenitor cells failing to respond to positional cues adopt non-myogenic fates in *myf-5* null mice. *Nature* **384**, 266-270.

Tajbakhsh, S., Rocancourt, D., Cossu, G. and Buckingham, M. (1997). Redefining the genetic hierarchies controlling skeletal myogenesis: *Pax-3* and *Myf-5* act upstream of *MyoD*. *Cell* **89**, 127-138.

Venters, S. J., Thorsteinsdottir, S. and Duxson, M. J. (1999). Early development of the myotome in the mouse. *Dev. Dyn*. **216**, 219-232.

Williams, B. A. and Ordahl, C. P. (1994). *Pax-3* expression in segmental mesoderm marks early stages in myogenic cell specification. *Development* **120**, 785-796.

Williams, B. A. and Ordahl, C. P. (1996). Manipulation of the avian segmental plate in vivo. In *Methods in Cell Biology, Vol 51*, vol. 51 (ed. M. Bronner-Fraser), pp. 81. San Diego, CA: Academic Press Inc.

Williams, B. A. and Ordahl, C. P. (1997). Emergence of determined myotome precursor cells in the somite. *Development* **124**, 4983-4997.

Williams, B. A. and Ordahl, C. P. (2000). Fate restriction in limb muscle precursor cells precedes high-level expression of MyoD family member genes. *Development* **127**, 2523-2536.

Williams, L. (1910). The somites of the chick. *Am. J. Anat.* **11**, 55-100.